

DETECTION OF FOREST FIRE, SMOKE SOURCE LOCATIONS IN KALIMANTAN DURING THE DRY SEASON FOR THE YEAR 2015 USING LANDSAT 8 FROM THE THRESHOLD OF BRIGHTNESS TEMPERATURE ALGORITHM

Kustiyo^{*)}, Ratih Dewanti, and Inggit Lolitasari
Remote Sensing Technology and Data Center, LAPAN

^{*)} e-mail: kustiyo@lapan.go.id

Received: 30 July 2015; Revised: 18 September 2015; Approved: 20 October 2015

Abstract. Almost every dry season, there are large forest/land fires in several regions in Indonesia, especially in Kalimantan and Sumatra in the dry season of August to September 2015 a forest fire in 6 provinces namely West Kalimantan, Central Kalimantan, South Kalimantan, Riau, Jambi, and South Sumatra. Even some parties proposed that the Government of Indonesia declares them as a national disaster. The low-resolution remote sensing data have been widely used for monitoring the occurrence of forest/land fires (hotspots), and mapping of burnt scars. The hotspot detection was done by utilizing the data of NOAA-AVHRR and MODIS data which have a lower spatial resolution (1 km). In order to increase the level of detail and accuracy of product information, this research is done by using Landsat 8 TIRS (Thermal Infrared Sensor) band which has a greater spatial resolution of 100 m. The purpose of this research is to find and to determine the threshold value of the brightness temperature of the TIRS data to identify the source of fire smoke. The data used is the Landsat 8 of several parts of Borneo during the period of 24 August to 18 September 2015 recorded by the LAPAN's receiving station. Landsat - 8 TIRS band was converted into brightness temperature in degrees Celsius, then dots in a region that is considered the source of the smoke if the temperature of each pixel in the region $> 43^{\circ}\text{C}$, and given the attributes with the highest temperatures of the pixels in the region. The source of the smoke was obtained through visual interpretation of the objects in the multispectral Natural Color Composite (NCC) and True Color Composite (TCC) images. Analysis of errors (commission error) is obtained by comparing the temperature detected by TIRS band with a visual appearance of the source of the smoke. The result of the experiment showed that there were detected 9 scenes with high temperatures over 43°C from the 27 scenes Kalimantan Landsat 8 data, which include 153 sites. The accuracy (commission error) of identification results using temperature $\geq 51^{\circ}\text{C}$ is 0%, temperature $\geq 47^{\circ}\text{C}$ is 10%, and temperature $\geq 43^{\circ}\text{C}$ is 30.5%.

Keywords: *Landsat 8, TIRS, brightness temperature, hotspots, source of smoke*

1 BACKGROUND

Almost every dry season, there are large forest/land fires in several regions in Indonesia, especially in Kalimantan and Sumatra. This particularly occurred in the dry season during August to September 2015 in 6 provinces, namely West Kalimantan, Central Kalimantan, South Kalimantan, Riau, Jambi, and South Sumatra. Even some parties proposed that the Government of Indonesia declares them as a national disaster.

The low resolution of remote sensing data have been widely used for monitoring the occurrence of forest/land fires (hotspots), and mapping of burnt scars. The hotspot detection was done by utilizing the data of NOAA-AVHRR and MODIS data which have lower spatial resolution 1 km. Zhang (2011) conduct a research on forest fire detection in China using NOAA/AVHRR, FY-series, MODIS, CBERS, and ENVISAT. While Veerachai (2009) and Giglio et al (2009) study on

Table 2-1: Landsat 8 acquired from 24 August to 18 September 2015

No	Scene_date	No	Scene_date	No	Scene_date
1	117057_130915	10	120059_020915	19	121059_240815
2	117058_130915	11	120059_180915	20	121060_090915
3	117059_130915	12	120060_020915	21	121060_240815
4	117060_130915	13	120060_180915	22	121061_090915
5	117061_130915	14	120061_020915	23	121061_240815
6	117062_130915	15	120061_180915	24	121062_090915
7	117063_130915	16	120062_020915	25	121062_240815
8	120057_020915	17	120062_180915	26	122059_310815
9	120058_180915	18	121059_090915	27	122060_310815

MODIS data application and its accuracy for detecting point location of a forest fire. Operational of near-real time MODIS temporal series at 1-km spatial resolution to detect forest fire was applied by Ichoku *et al.*, (2004) that mainly using the 4 μm and 11 μm MODIS channels to produce brightness temperature to measure the rate of emission of Fire Radiative Power (FRE) which is the MODIS fire product. Wang *et al.*, (2012) also use a composite of NDVI for a 16-day period to monitor the burnt scars for large scale. Recent method to detect burnt scars using sub-pixel (SPM) of MODIS conducted by Ling *et al.*, (2015) which aim to refine the accuracy of MODIS that in average produce information in 500 m.

On the other hand, research on utilizing high spatial resolution to map the burnt scars such as Landsat have also been conducted by several researchers. Jaya (2000) use Landsat TM imagery for identifying the location of burnt scars effectively and accurately using the multitemporal principal component. Identify burnt scars using several parameter such as Normalized Burn Ratio (NBR) and

Global Environmental Monitoring Index (GEMI) (Wiweka *et al.*, 2014; Picotte and Robertson 2011; Chen *et al.*, 2011; Roy *et al.*, 2006; Boer *et al.*, 2008 and Liu *et al.*, 2014) and Random Forest algorithm (Holden *et al.*, 2009), but these study solely using parameter derived from the multispectral Operational Land Imager (OLI) band. Another research use high temporal imagery and high spatial resolution imagery to map the burnt scars over 6 years in Boreal forest using MODIS-Terra and Aqua data and NOAA-AVHRR to tracked the fires within days which then classified using Bayesian network to detect the burnt scars, while the Landsat TM imagery solely used to inspect and provide the perimeter burnt scars accurately due to the higher detail resolution and validation of MODIS which using linear regression (Moreno-Ruiz *et al.*, 2014; Tsela *et al.*, 2010).

The Infra-Red sensor has the advantages to recording the radiation of Infra-Red reflected from the Earth's surface. Two types of Infra-Red sensor's wavelength, namely Medium Wave Infra-Red and Long Wave Infra-Red. This

radiation emitted from the object with warm temperature. Application on this band is for measuring soil and sea-surface temperature and also for detecting forest fire (Jaka, 2000).

The sensor recorded the total amount of radiation emitted in the wavelength depend on the particular range of temperature. This accordance with the Planck equation where the Earth was assumed as the black emitter comprises of various temperature, so as the object has a certain brightness temperature captured from the maximum EME radiation on a certain wavelength. For example, the Earth surface/object which has 300 K temperature brightness will have a peak radiation emitted at 10 meters and the peak in the certain wavelength will decrease steadily as the increasing of temperature. Therefore, the better accuracy for detecting the Earth's surface temperature in the thermal sensor is by using Infra-Red with 10 m resolution. Another advantage of utilizing the Infra-Red band for identification of forest burnt scars and hotspot such as a temperature of 500 K to >1000 K. The radiation emission peak detected at 3.8 meters.

Landsat 8 as a sun-synchronous satellite orbiting the Earth with the elevation of 705 km, 98.2° inclined, circled the Earth in 99 minutes with the revisit the same location in 16-day period (Sitanggang, 2010). Landsat 8 satellite operates two sensors, OLI and TIRS, comprises with 9 multispectral bands and 2 thermal bands. This satellite was built based on the development of its predecessor, which is Landsat-7 ETM+ (*Enhanced Thermal Mapper plus*). Therefore, this new generation of Landsat satellite series has new channels of wavelength where band 1 with the wavelength ranging from 0.433–0.453 μm is used for identification of aerosol and shore line, band 9 with the wavelength ranging from 1.360–1.390 μm is used for detecting cirrus clouds. While

other TIRS bands are for detecting brightness temperature of objects.

Since 2013, Landsat 8 satellite imagery can be acquired and processed in the Indonesian National Institute of Aeronautics and Space's (LAPAN) ground station. Therefore, with an existing abundance of Landsat 8 availability with the higher accuracy compare to the low-resolution data, this satellite offers continuity and complete spectral band, including thermal band which will benefit in supporting monitoring of forest burnt scars and detecting its point location of the smoke source accurately.

This research will detect the smoke source location from forest fire approached by the combination of the Operational Land Imager (OLI) with Thermal Infrared Sensor (TIRS) using Landsat 8 for spatial resolution in 100 meters. The accuracy assessment also was done by regression (Gallego, 2004) using visual investigation that correlated the temperature in the pixel and the percentage of accuracy.

Next, this methodology could be used to monitor burnt scars in near real time, and could be used as complement data or could be used as reference data to improve the previous methodology using coarse resolution such as MODIS and NOAA data.

This paper have been presented in National Seminar on Remote Sensing in Bogor 2015, that was organized by LAPAN, also it was published in the seminar proceedings, Kustiyo *et al.* (2015). Some modification and review was done especially in writing structure and language.

2 MATERIALS AND METHODOLOGY

2.1 Data, Location, and Software

The study area located in Kalimantan island where the Landsat 8 imagery acquired from LAPAN's ground station from 12 August to 18 September 2015. Detail of the 17 scene location from

27 different images date is provided in Table 2-1.

However, some of the areas in the Central Kalimantan were not covered by TIRS sensor during the period of the study, while the OLI data can be retrieved. The TIRS data will be used to derive brightness temperature and OLI will be used to assess the result visually.

To process the image such as displaying, and visually assess the result will be operated in the ErMapper 7.0, while the measurement of brightness temperature will be run in the C++ program.

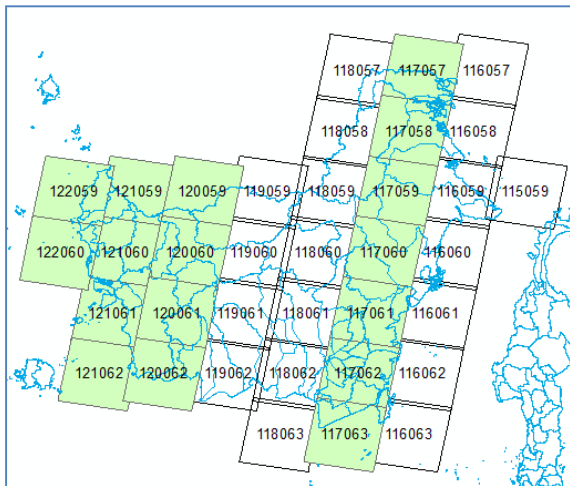


Figure 2-1: Distribution of Landsat 8 acquired from 24 August to 18 September 2015 that consist of full bands (OLI and TIRS) in green and OLI without TIRS in white.

2.2 Methods

In general, the flowchart of the study can be seen in Figure 2-2, where the steps of the study will be explained in this section.

The Landsat 8 Level-1 orthorectification data that used in the study composed of 2 types; (1) band 10 of TIRS and, (2) Red Green Blue (RGB) composite of true-color and natural-color. The TIRS band will be used to derive the brightness temperature, which the steps are explained below:

- Conversion of digital number (DN) to *Top Of Atmosphere* (TOA)

$$Radiance[i]=Gain[i] * Dn[i] + Offset[i] \quad (2-1)$$

Where:

i : band 10 or band 11 of TIRS

Gain, Offset: conversion constants as can be seen in Table 2-2.

- Conversion of TOA to brightness temperature

$$TB[i] = K2[i]/\log((K1[i]/Radiance[i] + 1) \quad (2-2)$$

Where:

i : band 10 or band 11 of TIRS

TB : Brightness temperature level in Kelvin;

K1, K2 : conversion constants as can be seen in Table 2-2

- Conversion from Kelvin to Celsius

$$TBC[i]=TB[i]-273 \quad (2-3)$$

Where:

i : band 10 or band 11 of TIRS

TBC : Brightness temperature in °C.

Table 2-2: Conversion constants to measure TOA and brightness temperature

	Band 10	Band 11
Gain	0.0003342	0.0003342
Offset	0.1	0.1
K1	774.89	480.89
K2	1321.08	1201.14

Source: Landsat 8 Data Documentation and Information

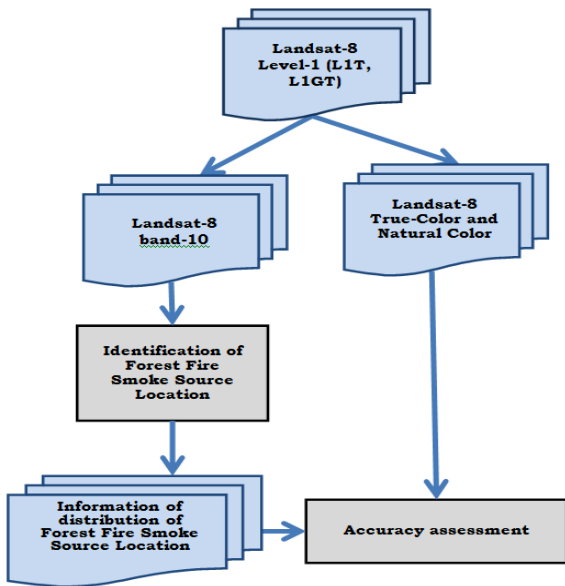


Figure 2-2: Workflow of method and analysis

The threshold which determined by calculation of brightness temperature in Celsius is then used to detect the central point location of the smoke source. It is assumed that temperature value ≥ 43 °C in the brightness temperature image is the potential for the occurrence of forest fire, smoke source, which then the pixel that predicted will be labeled in attribution.

The accuracy of the result is assessed based on visual analysis using multispectral Natural Color Composite (NCC) and multispectral True Color Composite (TCC). The error commission will be used to quantitatively measure the accuracy by comparing the area predicted as locations of forest fires, a smoke source from the thresholding result and the OLI images composited. Correlation of several point location predicted will be used to measure the level of the accuracy.

3 RESULTS AND DISCUSSION

3.1 Identification of forest fire smokes source location

Figure 3-1 represents the overlay between pixel predicted as forest fire smokes source location in a burnt scar area and the threshold of brightness temperature with temperature ≥ 43 °C. In

Figure 3-1, where the group of points located in the center of the polygon shows that the pixel has temperature ≥ 50 °C or higher than the pixel at the edge of the polygon that detected in the brightness temperature image. The highest temperature in the polygon colored with red points, while magenta points show that the pixel temperature ranging from 45-50 °C, the yellow points show that the pixel temperature ranging from 43-45 °C.

Thus can be assumed that the location of smoke source will be located in the center of the polygon with the highest temperature compared to the surrounding pixels, while the temperature will be decreased for the points that located away from the center or located at the border of the polygon or group of points.

The threshold of temperature can be used to predict the forest fire smoke source location which in this study is 43 °C. This obtained from several observations detected from composite images as seen in Figure 3-1. The Figure 3-1 also depicts the border line which located between burnt scars and vegetated areas. While the source of smoke pointed in the middle of the burnt scars. Yet, a lower value than the threshold < 43 °C will produce miss-identification or low accuracy in detecting the location of smoke.

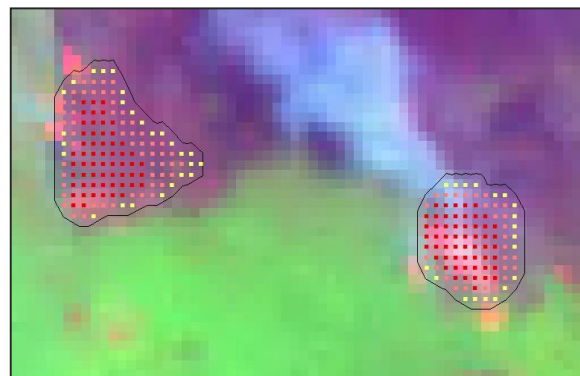


Figure 3-1: Pixel identified as smoke location (Red: > 50 °C; Magenta: 45°-50 °C; Yellow: 43°-45 °C)

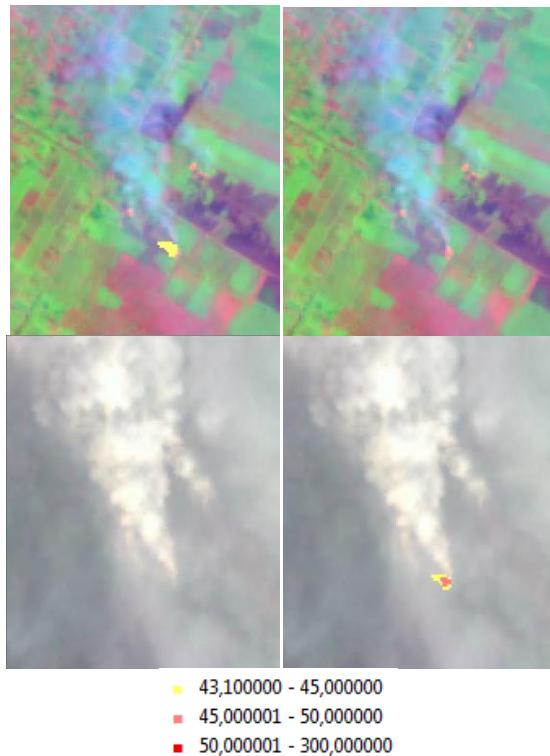


Figure 3-2: Identification of forest fire smoke source location in a composite true-color of OLI images showed in the images from left to right (a) and (b), while a composite of natural-color in (c) and (d). The image is overlaid with the points attribution of temperature level derived from brightness temperature of TIRS

Moreover, the area predicted as the forest fire smoke source can be seen clearly in Figure 3-2 using the composite image of NCC. However, the transition area or the land cover changes affected by this burnt scars such as from the vegetation area in a burnt scar area were difficult to be detected in this image composite. On the other hand, although the smoke depicted as a thin layer in true-color composite as in Figure 3-2 (a) and (b), the location of land cover change was clearly shown in this composite detected in the red area.

Therefore, this method which is derived from the combination analysis from the threshold of brightness temperature image and the two color composite images which are the NCC and

TCC provide a reliable information to detect the original location of the smoke. This method can also be applied in the others area in Indonesia in order to detect the central location of the forest fire smoke source.

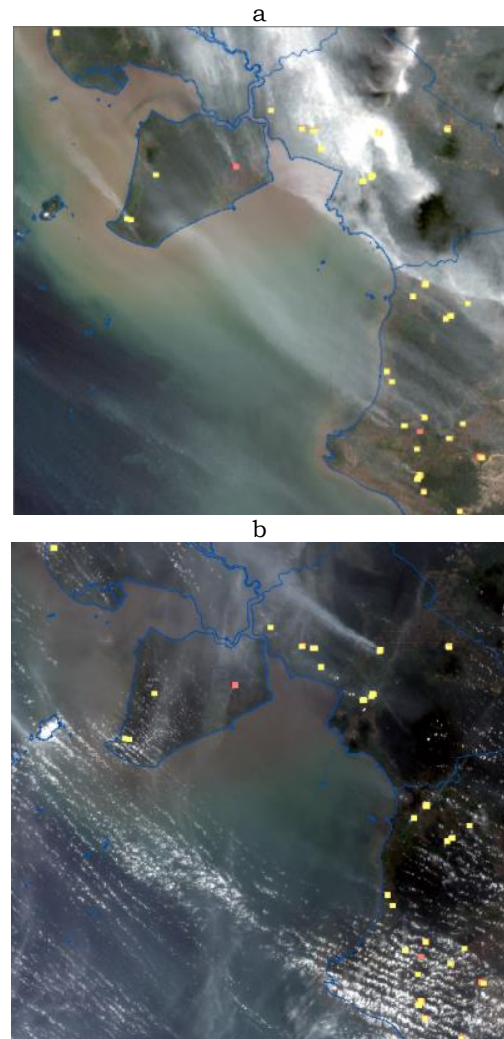


Figure 3-3: Distribution of the point's location of the source of the smoke in a burnt scar area located in scene 121061 with image date acquired at; (a) 9 September 2015, and (b) 24 August 2015

Another important to note in Figure 3-3 to identify the smoke is by detection of the shape. In Figure 3-3 where the points show the certain location of smoke in the TIRS images, although showed a thin appearance as shown in the composite image. This can also be highlighted that

smoke can be identified by the shape and the pattern which differ with clouds. For example, smoke identified by the shape that begins at one point with a white thick object in high elevation and followed by the spread shape that forms a long line and thinner at the tail which shows away from the central points, those affected by wind direction. While clouds identified by a thicker shape in the central and thinner at the surrounding edge.

Analysis of the 27 images that processed in 17 scene path/row Landsat 8, the study found that 9 scenes were contain offorest fire smoke source locations, while 8 scenes identified as clear/negative of smoke source locations. The smoke was largely founded in the west and south Kalimantan that shown in Figure 3-4, where 153 points were identified as the forest fire smoke source.

The area identified as the source of smoke location varied, based on the analysis, some of the areas contain of 2 pixels (0.18 hectares) to 882 pixels (79 hectares) with the average area of location were 56 pixels (5 hectares). However, the standard of the area affected by smoke may vary depend on the threshold, while a lower threshold will provide inaccuracy identification.

3.2 Accuracy Assessment

Visual accuracy assessment using TCC and NCC image composite of OLI band was used as a base to overlay the point's location to detect the forest fire smoke source location. Based on 153 points location of smoke in the threshold of 43 °C, the certain points were located in 105 points, while 46 points were negative of location that detected as the forest fire smoke source.

Based on Table 3-1, it can be seen that in the threshold of 43 °C, this will

produce an accuracy of 69.5%, while measuring using a tolerance deviation of 1 °C meaning that the certain accuracy obtained were 65%. More over to increase the accuracy to 90% will require the threshold in the brightness temperature image of 47 °C (Table 3-1 number 5) where from 66 points location, the points that detected at certain points were 59 points, while the 7 points identified as uncertain. This can also be concluded that an accuracy of 100% will be achieved in the threshold of 51 °C, this means that certain true smoke was located in the threshold ≥ 51 °C.

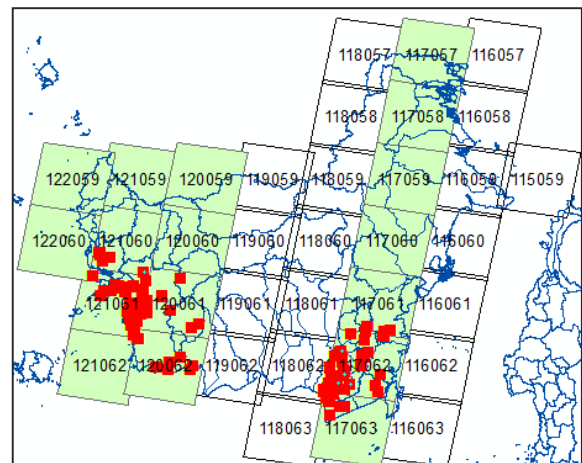


Figure 3-4: Distribution of pixel points location predicted as central of the smoke (red)

Table 3-1: Accuracy assessment derived from different threshold

No.	Temperature (°C)	Number of samples		Accuracy (%)
		False	True	
1	≥ 43	46	105	69,5
2	≥ 44	23	93	80,2
3	≥ 45	11	72	86,7
4	≥ 46	10	65	86,7
5	≥ 47	7	59	89,4
6	≥ 48	3	55	94,8
7	≥ 49	2	52	96,3
8	≥ 50	1	47	97,9
9	≥ 51	0	41	100,0

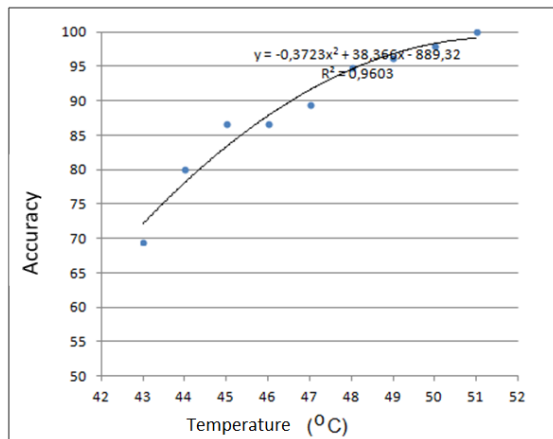


Figure 3-5: Correlation between brightness temperature threshold for detection of potential location of central of the smoke with its accuracy assessment

Based on the accuracy assessment resulted from different threshold in Table 3-1, the correlation between the accuracy and the points pixels in the brightness temperature that shown in Figure 3-5 meaning that this method has the correlation of accuracy $R = 0.96$ which modeled in the second order polynomial. While correlation in linear produced $R = 0.90$. The model shows that the accuracy to predict the location of forest fire smoke source (y%) can be achieved in which determined by the selection of threshold in the brightness temperature in x °C.

4 CONCLUSION

This research reveals that the method to predict the location of forest fire smoke source can be detected by combination analysis of brightness temperature threshold and composite image from Landsat 8 imagery to produce high accuracy information. Processed from 27 different image date from 17 path/row scene in Kalimantan show there were 153 points location which potential as the central location of smoke where 105 points were identified as the certain points and 46 were uncertain.

While the accuracy of the information shows that the threshold 43 °C will

produce 69.5% accuracy where 65% accuracy determined as the certain accuracy. The increase of the threshold to 47 °C will produce an accuracy of 90%, while the highest accuracy (100%) for detecting the central points location of smoke obtained for the threshold ≥ 51 °C. Thus the high correlation for the threshold of the brightness temperature image and accuracy measured using second correlation polynomial model resulted in $R = 0.96$. Therefore, this method can be applied to detect the potential location of central point's location of smoke in burnt scar area.

ACKNOWLEDGEMENT

The author would like to thank Division Chief of The Technology of System Acquisition and Ground Station in LAPAN and all the team members of the Landsat 8 data processing who have contributed by providing the Landsat 8 imagery level 1T and level-1GT as the main data, including to all of the team member in image processing division who processed the data.

REFERENCES

- Boer MM, Macfarlane C., Norris J., Sadler RJ, Wallace J., Grierson PF, (2008), Mapping Burned Areas and Burn Severity Patterns in the SW Australian Eucalyptus Forest using Remotely-Sensed Changes in Leaf Area Index. Elsevier Journal Remote Sensing of Environment 112: 4358-4369.
- Chen X., Vogelmann JE, Rollins M, Ohlen D., Key CH, Yang L., Huang C., Shi H., (2011), Detecting Post-Fire Burn Severity and Vegetation Recovery using Multitemporal Remote Sensing Spectral Indices and Field-Collected Composite Burn Index Data in a Ponderosa Pine Forest. International Journal of Remote Sensing 32(23): 7905-7927.

- Gallego FJ, (2004), Remote Sensing and Land Cover Area Estimation. *International Journal of Remote Sensing* 25(15):3019–3047.
- Giglio L, Loboda T, Roy DP, Quayle B, Justice CO, (2009), An active-fire based burned area mapping algorithm for the MODIS sensor. *Elsevier Journal Remote Sensing of Environment* 113(2): 408–420.
- Holden ZA, Morgan P., Evans JS, (2009), A Predictive Model of Burn Severity Based on 20-year Satellite-Inferred Burn Severity Data in a Large Southwestern US Wilderness Area. *Forest Ecology, and Management* 258(11): 2399–2406.
- Jaya INS, (2000), Technique for Detecting Forest Fire using Multitemporal Satellite Imagery: a Case in South Sumatera and Riau Province. *Journal of Tropical Forest Management* 6(2): 25-34. (In Indonesian)
- Kontoes C., (2013), Wildfire Rapid Detection and Mapping and Post-Fire Damage Assessment in Greece, Cited in http://www.earthzine.org/wildfire_rapid_detection_and_mapping_and_post-fire_damage_assessment_in_greece Earthzine.html. [Accessed 14 September 2013].
- Kustiyo, dan Dewanti R., 2015, Penentuan Ambang Batas Temperatur untuk Pendeteksian Sumber Asap Kebakaran Hutan/Lahan dari Data Landsat 8 (Studi Kasus Wilayah P. Kalimantan pada Musim Kemarau 2015),” in *National Seminar on Remote Sensing*, 652-660.
- Liew SC, (2001), Principles of remote sensing Cited in http://www.crips.nus.edu.sg/principles_of_remote_sensing - Centre for Remote Imaging, Sensing, and Processing, CRISP.
- Ling F., Du Y., Zhang Y., Li X., Xiao F., (2015), Burned-Area Mapping at the Subpixel Scale with MODIS Images. *IEEE Geoscience and Remote Sensing Letters* 12(9): 1963-1967.
- Liu Y., Dai Q., Liu J., Liu S., Yang J., (2014), Study of Burn Scar Extraction Automatically Based on Level Set Method using Remote Sensing Data. *PLoS ONE*, 9(2).
- Mazher A., Peijun L., Jun Z., (2012), Mapping Burned Areas from Landsat TM Images: A Comparative Study, *Computer Vision in Remote Sensing (CVRS) International Conference on*, 285-290.
- Moreno-Ruiz JA, Garc JR, Riaño D., Kefauver SC, (2014), The Synergy of the 0.05 (~ 5 km) AVHRR Long-Term Data Record (LTDR) and Landsat TM archive to map large fires in the North American Boreal Region from 1984 to 1998. *IEEE Journal of Selected Topics in Applied Earth Observations and Remote Sensing* 7: 1157-1166.
- Picotte JJ, Robertson KM, (2011), Validation of Remote Sensing of Burn Severity in South-Eastern US Ecosystems. *International Journal of Wildland Fire* 20(3):.453–464.
- Roy DP, Boschetti L., Trigg SN, (2006), Remote Sensing of Fire Severity: Assessing the Performance of the Normalized Burn Ratio. *IEEE Geoscience and Remote Sensing Letters* 3(1):112–116.
- Sitanggang G., (2010), Study of Utilization of Future Satellite: Satellite Remote Sensing Systems LDCM (Landsat 8). *Aeronautics and space magazine LAPAN* 11(2):47-58. (In Indonesian).
- Tanpipat V., (2009), MODIS Hotspot Validation over Thailand. *Remote Sensings Journal* 1(4): 1043-1054.
- Tsela PL, Helden PV, Frost P., Wessels K., Archibald S., (2010), Validation of the MODIS Burned-Area Products Across Different Biomes in South Africa. Paper presented at the *Geoscience and Remote Sensing Symposium (IGARSS)*, IEEE International.
- USGS, (2015), Landsat 8 Data Documentation and Information, Available at http://landsat.usgs.gov/Landsat_Processing_Details.php. [Accessed 16 October 2015].
- Wang J., Zhang W., Zhang Z., Wen Q., (2012), Burned Area Extraction Based on Time-Series Modis 250m NDVI of Guangxi

- Province, Earth Observation and Remote Sensing Applications (EORSA), Second International Workshop on, 8-11 June 2012, 166-170.
- Wiweka, Suwarsono, Nugroho J T, Arifin S., (2014), Performance Test Parameters of Remote Sensing for Identification Burned Area using Landsat 8. ICT For Smart Society (ICISS), International Conference on, 24-25 Sept., 2014, 91-100.
- Zhang JH, (2011), Detection, Emission Estimation and Risk Prediction of Forest Fires in China using Satellite Sensors and Simulation Models in the Past Three Decades - An Overview. International Journal of Environmental Research and Public Health 8(8): 3156-3178.